Simple and efficient inverse hysteretic model and associated experimental procedure for precise piezoelectric actuator control and positioning

Mickaël Lallart, Kui Li, Zhichun Yang, Shengxi Zhou, Wei Wang

Simple and efficient inverse hysteretic model and associated experimental procedure for precise piezoelectric actuator control and positioning

Mickaël LALLART[1,2,*], Kui LI[1], Zhichun YANG[1], Shengxi ZHOU[1] and Wei WANG[1]

[1] *School of Aeronautics, Northwestern Polytechnical University, XI'AN, People's Republic of China*
[2] *Univ. Lyon, INSA-Lyon, LGEF EA682, F-69621 VILLEURBANNE, France*

Abstract

This paper exposes inversion techniques of a simple yet efficient system-level approach for modeling quasi-static hysteretic behavior of piezoelectric actuators, allowing the transducer voltage to be properly shaped to get the desired target strain response. The inversion principles lie in considering a coefficient relating the voltage derivative to the target strain derivative through a simple formulation using a function of the input strain, combined with equivalent strain cancellation and inversion when the desired target strain derivative crosses zero value. Conceptual and theoretical developments are validated through experimental measurements that show good control capabilities of the quasi-static strain. Hence, the proposed concept provides a lightweight yet efficient approach for embedded control systems.

Keywords: hysteresis, actuator, piezoelectric, control, inverse model

1. Introduction

The rise of electroactive devices and associated smart materials and structures has unveiled the development of numerous control systems for ensuring proper response of structures with respect to their application environments (control, sensing, positioning or vibration control for instance - [1, 2, 3, 4, 5, 6]). Nevertheless, actuators may not exhibit a perfect linear response to input stimulus and are even hysteretic in most cases ([7, 8, 9, 10]), yielding quite complex implementation. Therefore, control systems should be able to adapt to these non-ideal behaviors, while being as simple as possible in order to be easily implementable in lightweight controllers with limited computational abilities and memory in the framework of embedded systems.

Classical hysteresis modeling approaches may typically be decomposed into two classes ([11]). The first family, conceptually close to the material behavior (in terms of domain switching for example), lies in considering several unit elements ("*hysterons*") that, when put together, allow relating the global transducer behavior. This class of hysteresis models includes the well-known Preisach model ([12]) and its derivatives ([9, 13, 14, 15]) as well as Maxwell-slip and dry friction-

*Corresponding author - mickael.lallart@insa-lyon.fr

based approaches ([16, 17, 18]). The second kind of models lies in mathematical formulation based on physical analysis or phenomenological approach, such as Jiles-Atherton ([19, 20, 21]), Bouc-Wen ([22, 23, 24]), Duhem models ([25, 26, 27]) or more recently the NARMAX method (*Nonlinear AutoRegressive Moving Average model with eXogenous inputs* - [28]). Each class of these hysteresis models has its own advantages and drawbacks: while being able to closely match the transducer response, hysteron-based formulations, requiring a relatively large amount of unit elements, are computationally intensive which may compromise their effective implementation in lightweight controllers for embedded systems for instance. On the other hand, mathematical function-based approaches are much lighter and require a reduced parameter set, but may fail in representing particular behaviors such as minor loops and could feature stability issues as well.

In order to provide a trade-off between computational efforts and accurate representativeness of a transducer's response, a system-level approach inspired from the strain-electric field butterfly shape at the material level has recently been introduced in [29]. The model basics lie in the definition of a output derivative-input derivative coefficient (*e.g.*, voltage-dependent strain derivative over voltage derivative coefficient for a piezoelectric transducer) using a mathematical function that is shifted and reversed, both along the x-axis (*i.e.*, voltage in the case of a piezotransducer) when the input signal (voltage) derivative crosses zero value[1]. Such a model therefore allows simple implementation (requiring 1 memory quantity - representing the remanence - and typically 2 or 3 fixed parameters) while being able to take into account particular behaviors such as actuator minor loops.

Meanwhile, in terms of hysteretic actuator control, many works have been devoted to the use of one or the other kind of hysteresis models. Nevertheless, the principles for ensuring proper response of the transducer with respect to the target value is typically done in two ways (without consideration of neural network-based approaches that may not be implementable in lightweight, embedded systems). First, the hysteresis effect may be compensated by including a direct model of the actuator in the control loop (either feedforward or feedback), using inverse multiplicative structure ([30, 31]) for example. While these approaches may be quite simple to implement when the direct hysteretic model is available, they may yield high computational cost as well as robustness and stability issues. Hence, the other method lies in directly inverting the direct hysteresis model, hence directly giving the control signal to get the desired transducer response ([32, 33, 34, 35]). While being more efficient, the latter technique cannot be strictly applicable to all of the hysteresis models (especially in an analytical fashion) thus requiring approximated functions ([36]), or yields computationally and memory-intensive approaches (*e.g.*, look-up tables). Other approaches than these two classical ones also exist, such as tracking error bounding ([37]). Although robust with respect to the hysteretic behavior of the transducer, such approaches are still usually

[1]While the model principles allow to consider any derivative, it will be considered in the followings that the derivation variable is the time.

computationally-intensive and their implementation in lightweight controllers may be an issue.

Still, inversion techniques are facing a trade-off between computational requirements and accuracy. Hence, the purpose of this study is to expose and devise the inverse approach of the direct system-level model presented in [29] for the control of a piezoelectric transducer, providing a computationally efficient yet accurate way for controlling the mechanical output of the actuator. The motivation behind such an analysis lies in that fact that the direct hysteretic model, although allowing a quite precise prediction of the actuator response to an electrical stimulus, cannot be directly and readily applied for controlling the actuator with a desired input strain (including it in a compensation loop would lead to a quite computationally-intensive technique possibly featuring robustness issues), while an inverse model takes directly the target strain as direct input. Hence, the originality of this present study with respect to this previous model ([29]) yields in the direct disposal of a method able to automatically set the required voltage to reach the desired target strain in quasi-static hysteretic actuators, without the need of using complex methods based on direct actuator models. The inversion strategies are twofold for obtaining such a readily applicable control technique. First, an analytical inverted model will be presented when the function describing the output derivative-input derivative coefficient of the direct model is simple (linear). Then, the generalization to any kind of function, based on experimental procedures, will be exposed. It will be shown that one strength of the inverted model approach is that its generalization is based on similar principles than the direct model, considering the coefficient linking the input quantity derivative to the output one.

The paper is organized as follows. Section 2 recalls the main basics of the direct model, and introduces the concepts and theory for the inverse approach, with an example of analytical inversion given in Section 3. Then, Section 4 will present, in a pragmatic and applicative point of view, the use of the inverse model for more complex functions. Before final conclusions in Section 6, experimental and numerical investigations in terms of control will be exposed in Section 5 to validate the model and show its effectiveness.

2. Theoretical Modeling

2.1. Direct model basics

The principles of the direct approach described in [29] lie in describing the strain S-voltage V relationship through the voltage-dependent coefficient $\alpha(V)$ linking the strain derivative to the voltage derivative as:

$$S(t) = \int_{-\infty}^{t} \alpha\left(V\left(\tau\right)\right) \frac{\mathrm{d}V\left(\tau\right)}{\mathrm{d}\tau} \mathrm{d}\tau \tag{1}$$

where t refers to the time variable for instance (the model can however be applied as a function of any variable).

Hence, through the proper shaping of the voltage-dependent strain derivative-voltage derivative coefficient $\alpha(V)$, the actuator response may be obtained. More particularly, hysteretic response may be achieved by defining $\alpha(V)$ through a mathematical function h as well as introducing a variable shifting voltage V_{shift} for relating the hysteretic behavior as:

$$\alpha(V) = \alpha_0 + h\left(V - V_{shift}\right) \tag{2}$$

with α_0 representing the linear, low-voltage coefficient. V_{shift}, actually representing the hysteretic remanence / memory effect, is therefore a piecewise function defined in continuous time domain re-evaluated to the actual voltage value when the derivative of the latter crosses zero value:

$$\begin{aligned} \forall t \in [t_k; t_{k+1}[: \quad & \tfrac{\mathrm{d}V}{\mathrm{d}t}(t_k) = 0 \wedge \tfrac{\mathrm{d}V}{\mathrm{d}t}(t_{k+1}) = 0 \\ & \wedge \tfrac{\mathrm{d}V}{\mathrm{d}t}(t \neq t_k) \neq 0 \Rightarrow V_{shift}(t) = V(t_k) \end{aligned} \tag{3}$$

with t_k and t_{k+1} representing the time instants when this piecewise constant function changes its value[2]. In other words, V_{shift} is set to the voltage extremum value until the next one occurs. As an example, Figure 1(a) depicts both the evolution of $\alpha(V)$ and strain as a function of applied voltage.

2.2. Inverse model principles

The previous model linking the strain to the applied voltage may be useful for predicting the voltage-induced strain of a piezoelectric actuator for instance. However, being able to directly get the required voltage to obtain a desired target strain is of particular interest in an applicative point of view for control systems. Although compensation techniques can be applied with the direct approach, the novelty of the present study is to propose to inverse this direct model in order to dispose of a straightforward implementation, hence requiring less computational efforts while being less prone to error.

To do so and in a similar way than the direct model, a coefficient $\beta(S)$, this time linking the voltage derivative to the strain derivative as a function of the strain, is introduced as:

$$\beta(S) = \frac{\mathrm{d}V}{\mathrm{d}S}(S) \tag{4}$$

Using the same example as previously (Figure 1) but representing $\beta(S)$ yields the curves shown in Figure 1(b). From these results, it can be seen that a similar procedure than the direct model can be applied by reversing the input/output quantities (*i.e.*, voltage and strain), highlighting the advantage of the system-level approach in terms of versatility.

Hence, considering an input target strain S, the procedure of the inverse model consists in defining the voltage as:

[2]Note that Eq. (3) is only valid for $\mathcal{C}^1$ functions. While this condition may not be respected for pure theoretical signals, practical implementation does not suffer from this limitation.

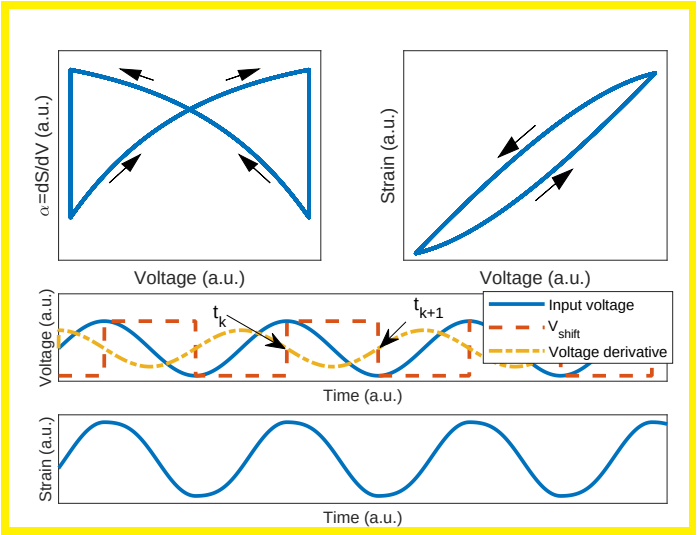

(a) Original direct $V - S$ model

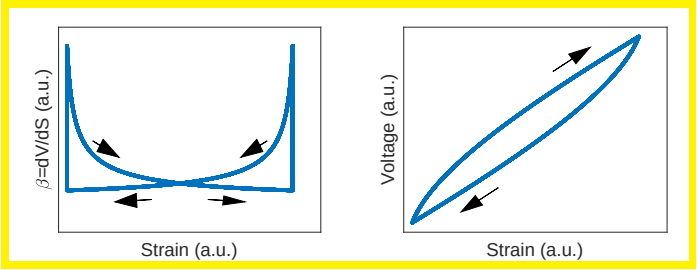

(b) Inverse $S - V$ model

Figure 1: Original direct and proposed inverse model principles.

$$V(t) = \int_{-\infty}^{t} \beta\left(S\left(\tau\right)\right) \frac{\mathrm{d}S\left(\tau\right)}{\mathrm{d}\tau} \mathrm{d}\tau \tag{5}$$

where the coefficient $\beta(S)$ is defined by:

$$\beta(S) = \beta_0 + h'\left(S - S_{shift}\right) \tag{6}$$

with S_{shift} representing the shifting/memory strain that is obtained when the target strain derivative crosses zero value:

$$\begin{aligned} \forall t \in [t_k; t_{k+1}[: \quad & \tfrac{\mathrm{d}S}{\mathrm{d}t}\left(t_k\right) = 0 \wedge \tfrac{\mathrm{d}S}{\mathrm{d}t}\left(t_{k+1}\right) = 0 \\ & \wedge \tfrac{\mathrm{d}S}{\mathrm{d}t}\left(t \neq t_k\right) \neq 0 \Rightarrow S_{shift}(t) = S\left(t_k\right) \end{aligned} \tag{7}$$

(as previously, S_{shift} can be also be defined as the strain extremum value until the next one occurs) and h' is the hysteresis-defining function that shares similar properties than h:

(i) for a symmetric hysteretic behavior, h' is even, and the expression of β can be rewritten as a function of another function g' only defined for positive reals as $\beta(S) = \beta_0 + g'\left(|S - S_{shift}|\right)$

(not that taking into account asymmetric behavior consists in defining h' not even, with the the positive part relating the ascending branch and the negative one the descending one)

(ii) h' can be set as $h'(0) = 0$ so that the linear, low strain response is represented by β_0. Although not required, setting both $h(0)$ and $h'(0)$ to 0 yields $\beta_0 = 1/\alpha_0$.

2.3. Direct and inverted model relationship

The previous section demonstrated that a similar approach than the direct model can be considered to get the voltage-strain relationship, or in other words to compute the required driving voltage to obtain the desired target strain. This section aims at giving some insights in terms of direct and inverse model link. Starting from the respective definition of the strain derivative-voltage derivative coefficient $\alpha(V')$ of the direct model and the voltage derivative-strain derivative coefficient $\beta(S')$ of the inverse model given by:

$$dS = \alpha(V')dV' \tag{8}$$

$$dV = \beta(S')dS' \tag{9}$$

where S and V respectively stand for the output strain in the direct model and the required command voltage for the inverse model and V' and S' the input voltage (direct model) and target strain (inverse model), respectively, inserting Eq. (8) into Eq. (9) and equalizing both strains and voltages yields the following relationship between the coefficients α and β:

$$dV = \beta(S')\alpha(V')dV \Rightarrow \alpha(V') = \frac{1}{\beta(S')} \tag{10}$$

However, α is here a function of the target strain S' and β of the input voltage V'. In order to obtain an expression of the same input quantity, namely the desired target strain S', it is nevertheless possible to use Eq. (9) considering $V = V'$, yielding:

$$\alpha\left(\int_{S'_{init}}^{S'} \beta(S')dS'\right) = \frac{1}{\beta(S')} \tag{11}$$

where S'_{init} represents the initial strain.

3. Experimental investigation of an analytical inversion example

3.1. Analytical derivation

From the link between the direct and inverse models, it is proposed here to analytically derive the relationship between the two models in the simple case of a linear expression for $\alpha(V')$:

$$\alpha(V') = \alpha_0 + \gamma V' \tag{12}$$

where γ represents the linear slope of the strain derivative-voltage derivative coefficient.

Hence, applying Eq. (11) with the previous expression leads to:

$$\alpha_0 + \gamma \int_{S'_{init}}^{S'} \beta(S')dS' = \frac{1}{\beta(S')} \tag{13}$$

The solution of Eq. (13) has the following form:

$$\beta(S') = k\,(S' + \sigma)^p \tag{14}$$

giving, when inserted into Eq. (13):

$$\alpha_0 + \frac{\gamma k}{p+1}\left[(S'+\sigma)^{p+1} - (S'_{init}+\sigma)^{p+1}\right] = \frac{1}{k}\,(S'+\sigma)^{-p} \tag{15}$$

Identifying the parameters p and k from the left and right sides of the previous equation therefore gives the following values:

$$\begin{array}{rcl} p+1 = -p & \Rightarrow & p = -\frac{1}{2} \\ \frac{\gamma k}{p+1} = \frac{1}{k} & \Rightarrow & k = \sqrt{\frac{1}{2\gamma}} \end{array} \tag{16}$$

that then allows obtaining the strain shift parameter σ when combined with the initial strain S_{init} as:

$$\sigma = \frac{{\alpha_0}^2}{2\gamma} - S'_{init} \tag{17}$$

Finally, the expression of $\beta(S')$ is solved from the parameters describing the coefficient $\alpha(V')$ and from the initial strain S'_{init}:

$$\beta(S') = \sqrt{\frac{1}{2\gamma\,(S' - S'_{init}) + {\alpha_0}^2}} \tag{18}$$

3.2. Experimental assessment

Figure 2 depicts the reconstructed input voltage from experimentally obtained strains under sinusoidal voltage excitation and from the identified parameters for the function α ($\alpha_0 = 6.4$ μdef.V^{-1} and $\gamma = 0.08$ μdef.V^{-2} - [29]). The test apparatus consisted in a PI$^{\text{TM}}$ *PICMA*® *P-888.51* stack actuator (with input voltage in the range of $0-100$ V) equipped with a strain gauge ($BQ120-3CA$ from Zhonghang Electronic Measuring Instruments Co., LTD - nominal resistance value of 120.3 Ω) connected to a quarter Wheatstone bridge and conditioner (Donghua Testing Technology Co., LTD $DH3840$) for strain measurement. Strain sampling rate was set to 1 ms, and the signal was then post-processed using a 5-point moving average filter.

Hence, it can be seen that the voltage reconstruction matches well the actual voltage applied during the experiment, although slight underestimation can be observed for high voltages (reaching a relative absolute error of 6% with respect to the experimental voltage magnitude). These

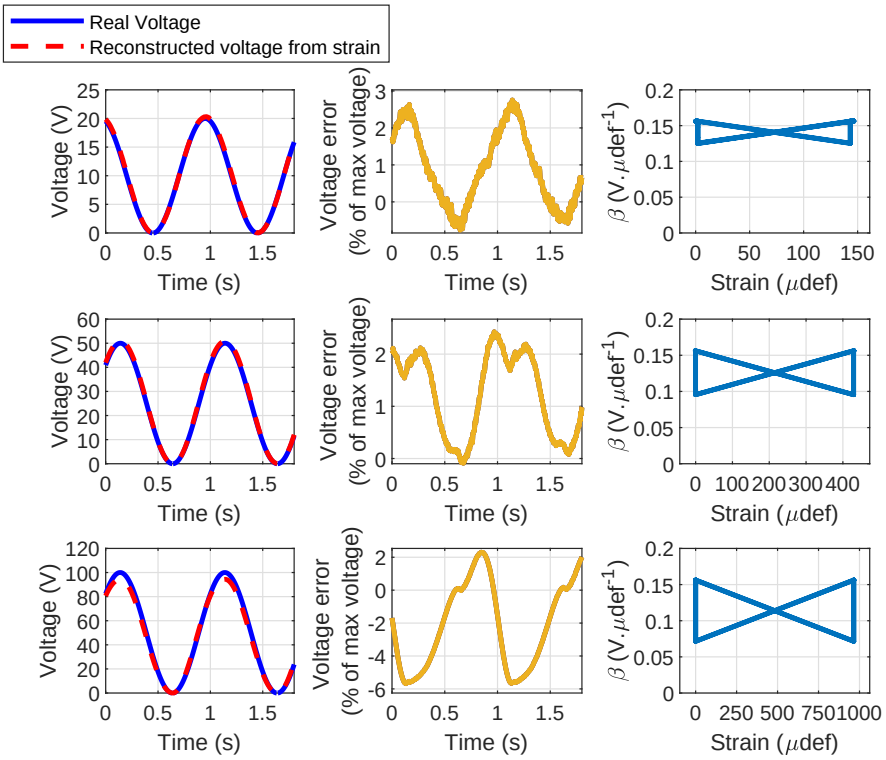

Figure 2: Voltage reconstruction from experimental strain using inversion of linear model ($\alpha_0 = 6.4$ μdef.V^{-1} and $\gamma = 0.08$ μdef.V^{-2}).

discrepancies can however be explained by the limit of the linear approximation for the function h in describing the strain derivative-voltage derivative coefficient $\alpha(V')$[3].

4. The Experimental Way

The analytical expression linking the direct and inverse models, Eq. (11), may not be practical and even impossible to solve for some forms of α. Hence, this section provides a more convenient way for obtaining the required voltage derivative-target strain derivative coefficient β. The principles are based on an experimental identification procedure quite similar to the direct model ([29]). More specifically, the procedure is as follows:

1. Application of a voltage V to the transducer and recording of the measured strain S.

2. Computation of strain and voltage derivatives[4] (dS and dV respectively) and calculation of $\beta = \mathrm{d}V/\mathrm{d}S$.

3. Representation of $\beta(S)$ as a function of the strain S and curve fitting.

[3] In [29], an exponential function for α is shown to provide a better fit.

[4] for example time-domain derivatives, or directly differentiation of strain and voltage vectors in discrete case.

When doing so, the experimental curves (still considering PI™ *PICMA*® *P-888.51* stack actuator with $BQ120-3CA$ strain gauge and $DH3840$ signal conditioner) giving the coefficient β for ascending and descending strains considering several voltage magnitudes are depicted in Figure 3(a). In order to remove part of the noise that arises from the derivation/differentiation process, all signals were downsampled by a factor of 20 and were cropped (by 3, 2 and 1 samples for driving voltage magnitudes of 20 V, 50 V and 100 V respectively) to remove the derivation/differentiation divergence due to low strain rate close to minimum and maximum values. First, results demonstrate that the shape of β is consistent with the butterfly-shape assumption and expected model behavior (Figure 1(b)). Secondly, it is possible to properly fit the coefficients. More particularly, bi-exponential fit in the form of:

$$\beta(S) = \eta_1 e^{\nu_1|S-S_{shift}|} + \eta_2 e^{\nu_2|S-S_{shift}|} \tag{19}$$

is considered for analytically describing the evolution of β. It can be noted that the use of exponential functions can be found in other works related to hysteretic actuator modeling for control purposes, such as in [38] that consisted in charge-voltage (or current-voltage) mapping for obtaining the hysteretic response. In the present study, the bi-exponential fit is shown to follow quite well the evolution of the coefficient for all of the considered driving voltage magnitudes, as demonstrated in Figure 3(b) for ascending strains, although inverse linear approach seems to be slightly better adapted to medium excitation magnitude case. It should be noted here that the considered curves were all obtained considering an zero initial voltage. In the considered approach however, as the effective strain (target one minus shift) is reset at each extremum, so is the value of β and thus the slope. While this slope is not the same than the one at the considered strain value for nonlinear functions (allowing relating minor loops), the fact that the initial slope remains the same yields minor loops with same gains. However, it has been demonstrated that a slight modification

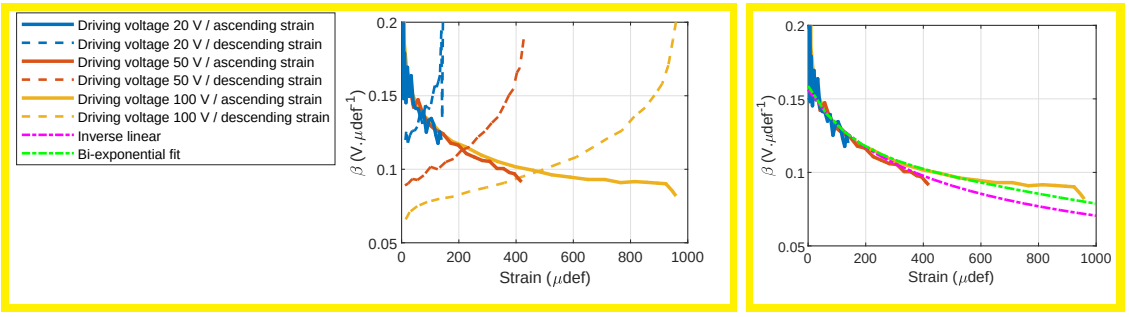

(a) Experimental value of β as a function of strain (both ascending and descending strain)

(b) Fit considering ascending strain only

Figure 3: Experimental plots of the voltage-strain derivative coefficient and comparison with inverse linear model and bi-exponential fit ($\eta_1 = 0.04036$ $V.\mu\text{def}^{-1}$, $\nu_1 = -7.789 \times 10^{-3}$ μdef^{-1}, $\eta_2 = 0.1184$ $V.\mu\text{def}^{-1}$ and $\nu_2 = -408.2 \times 10^{-6}$ μdef^{-1}).

of this gain arises with the bias ([39]). Such an effect is thus actually not taken into account by the proposed model and provides a way for enhancement[5].

Using such an approach, reconstructed voltage from measured strain is shown in Figure 4. It can be noted that, compared to the fitting procedure in Figure 3, parameters of the bi-exponential function have been slightly changed for better results, especially for low and medium excitation cases. Compared to inverse linear case, similar results in the low/medium range are observed, with slight high overestimation in this last case, but a significant improvement in the large voltage range is achieved. Interestingly however, it can be noted that the maximal relative error (with respect to the voltage magnitude) is quite constant and around 3% whatever the considered voltage magnitude.

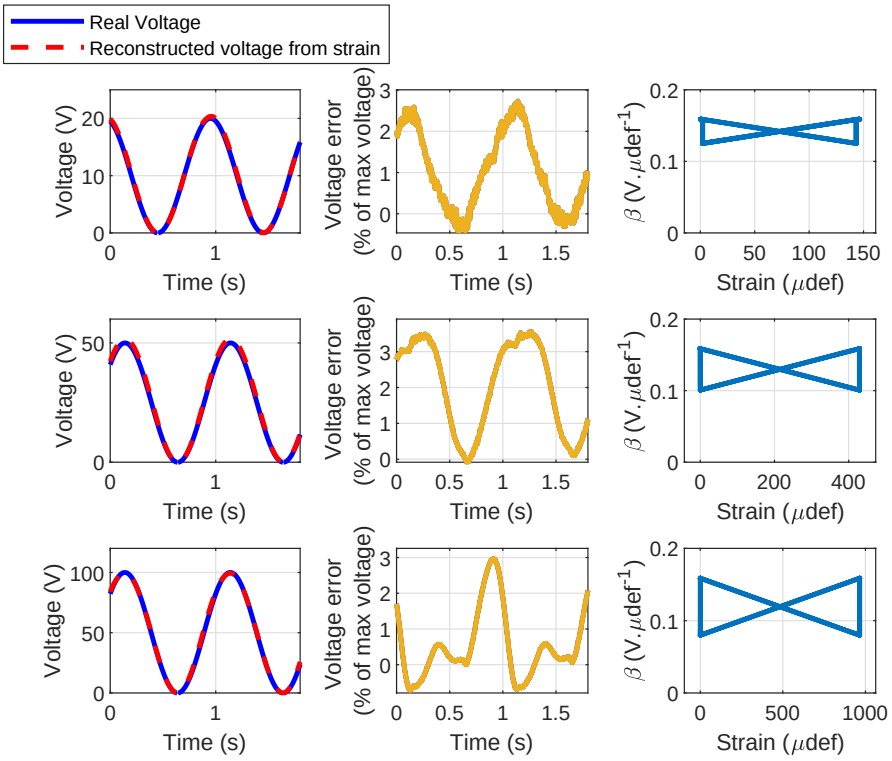

Figure 4: Voltage reconstruction from experimental strain using bi-exponential fit ($\eta_1 = 0.078\ V.\mu\text{def}^{-1}$, $\nu_1 = -5.916 \times 10^{-3}\ \mu\text{def}^{-1}$, $\eta_2 = 0.1000\ V.\mu\text{def}^{-1}$ and $\nu_2 = -277.8 \times 10^{-6}\ \mu\text{def}^{-1}$).

[5] Although out of the scope of the present study, using a second shifting variable, related to the first one (S_{shift}) is a probable way for taking into account variable minor loop gain, at the cost of a slight increase in complexity and memory and computational requirements.

5. Experimental Validation - Application to Linear Control of a Hysteretic Piezoelectric Actuator

5.1. Set-up & identification

The aim of the inverse model is to provide a mean of efficiently controlling, in quasi-static fashion, a transducer without relying on computationally and memory intensive compensation techniques for instance. Hence, this section aims at experimentally validating the possibility of effectively obtaining target strain output using the proposed model. To do so, the previous apparatus (PI™ *PICMA*® *P-888.51* stack actuator with $BQ120-3CA$ strain gauge and $DH3840$ conditioner) is still considered. The control voltage is generated by a dSpace© $DS2102$ control system (with a time step fixed to 0.1 ms) connected to a power amplifier (PI™ *E-503* Piezo Amplifier Module). The set-up schematic is depicted in Figure 5. It can be noted that the input strain to the dSpace system is only used for visualization and recording, and does not provide any feedback to the model block. Finally, preliminary measurements allowed identifying the control system parameters, either considering direct control (*i.e.*, assuming ideal linear relationship between strain and voltage), linear strain derivative-voltage derivative coefficient α (with β obtained through the analytical inversion exposed in Section 3), or bi-exponential function for β. Identified parameters are listed in Table 1.

5.2. Control implementation

In order to generate the proper control voltage to get the desired target strain using the previous model, the dSpace system (still with a time step of 0.1 ms) is this time fed with the Simulink® schematics depicted in Figure 6, for both the inverted linear direct model and bi-exponential inverse expression of the voltage derivative-strain derivative coefficient β (these schematics correspond to the block labeled *"Inverse model"* in Figure 5). In this study, only open-loop control is considered, to clearly demonstrate the relevance of the proposed scheme. Input is the target (desired) strain and

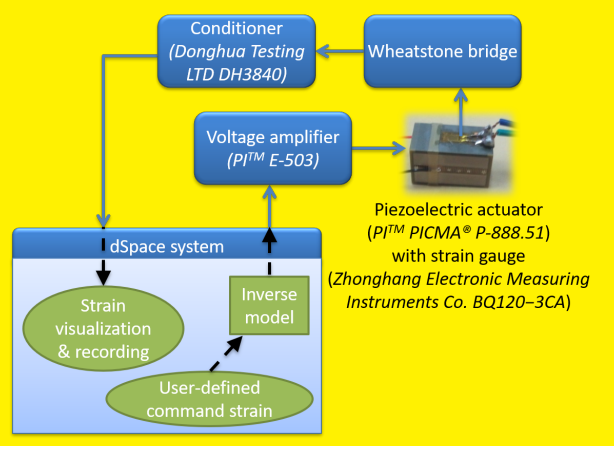

Figure 5: Experimental set-up.

Direct control - $\beta(S) = \beta_{direct}$	
Control gain β_{direct}	$\frac{1}{12}$ V.μdef^{-1}
Inverse linear model - $\beta(S) = \sqrt{\frac{1}{2\gamma\lvert S-S_{shift}\rvert+{\alpha_0}^2}}$	
Low-voltage strain-voltage derivative coefficient α_0	6.2 μdef.V^{-1}
Slope coefficient γ	0.075 μdef.V^{-2}
Bi-exponential inverse model - $\beta(S) = \eta_1 e^{\nu_1\lvert S-S_{shift}\rvert} + \eta_2 e^{\nu_2\lvert S-S_{shift}\rvert}$	
First pre-exponential factor η_1	0.078 V.μdef^{-1}
First exponential coefficient ν_1	-5.916×10^{-3} μdef^{-1}
Second pre-exponential factor η_2	0.100 V.μdef^{-1}
Second exponential coefficient ν_2	-277.8×10^{-6} μdef^{-1}

Table 1: Experimental model parameters.

the output is the associated voltage to experimentally reach such a strain. The principles consist in sampling the desired strain value when its derivative crosses zero value thanks to a zero-crossing detection block combined with a switch. Then this sampled target strain value, corresponding to S_{shift}, is subtracted from the target strain S. This effective strain $S - S_{shift}$ is then fed into the function describing $\beta(S)$ (block "$f(u)$" in Figure 6), yielding the current value of β. The strain derivative is then multiplied by the obtained coefficient, and the resulting variable integrated to get the required control voltage to obtain the target strain. In the following experiments, the desired test strain is set to be a sinusoidal signal of 1 Hz (for which the piezoelectric stack shows quasi-static response) with varying magnitude and shifted to yield unipolar driving.

5.3. Results & discussion

Figure 7 depicts the measured strain vs. the target one for the three considered control approaches (direct, inverse of linear model, bi-exponential inverse model) as well as the relative error with respect to the maximal command strain for each case. Hence, it can be observed a strong hysteretic response in the direct control, along with significant underestimation of the required voltage to achieve the target strain at low magnitude and significant overestimation at high strain magnitude. Therefore, such a control is not useable in practice. The inversion of the linear model permits much better response, with matching maximal strains with respect to the target one and reduced hysteretic response. Interestingly, the proposed approach performs better at high strain/voltage in

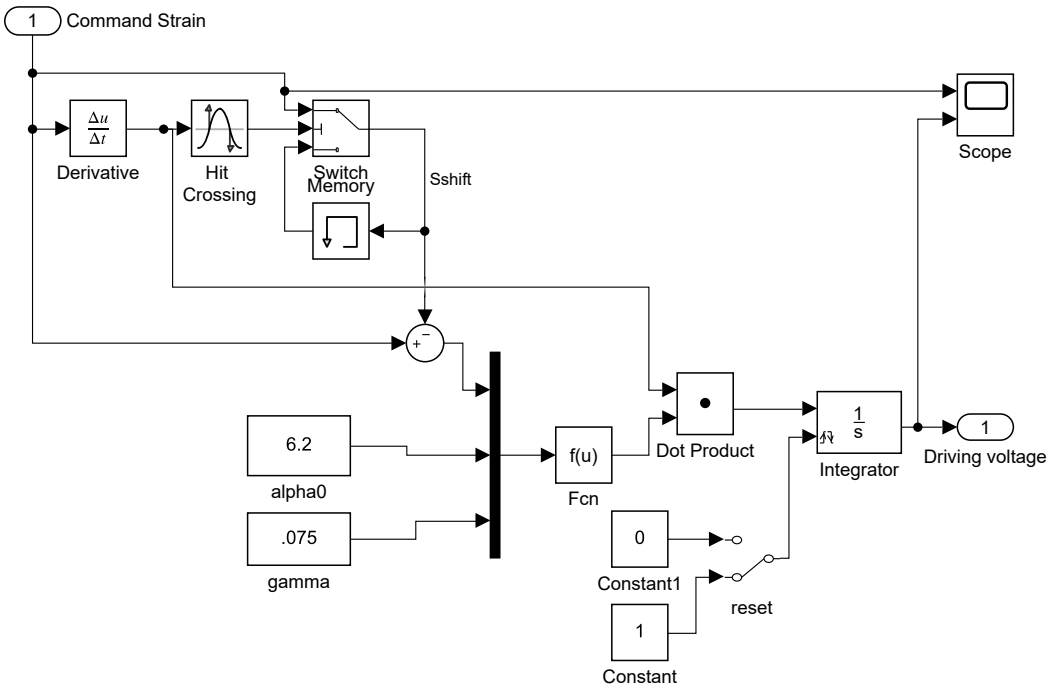

(a) Inversion of linear behavior

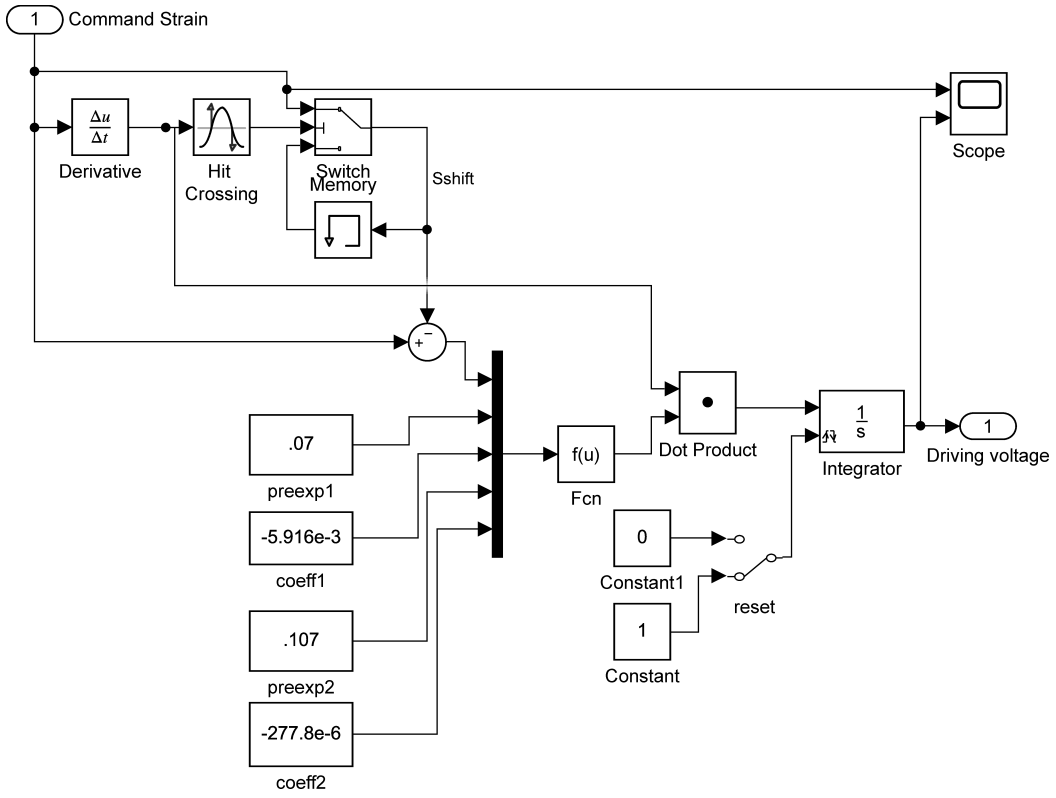

(b) Bi-exponential inverse behavior

Figure 6: Simulink schematics used in the experiment for modeling inverse hysteresis model (the integrator reset is used when the system is at rest to reinitialize the algorithm in the case of failure in the experiment, such as dSpace input voltage clipping).

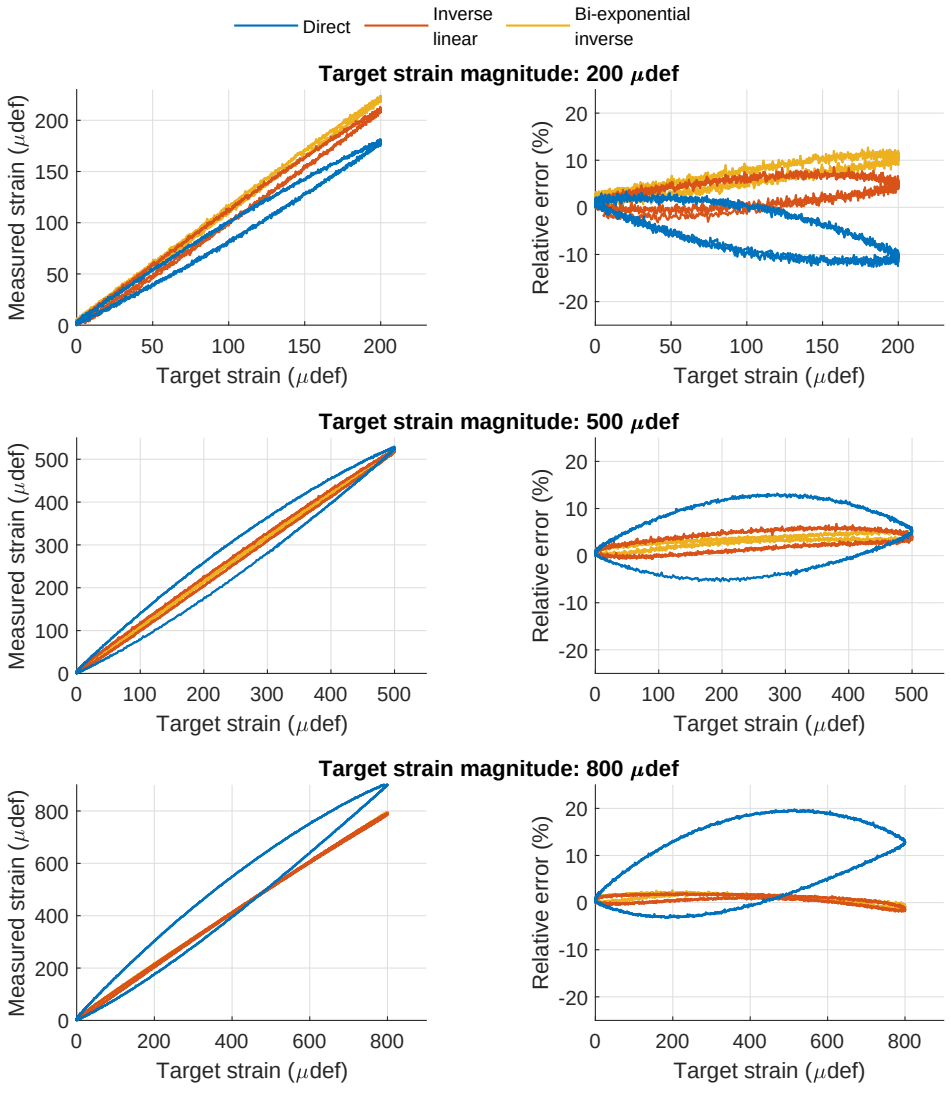

Figure 7: Experimental strain vs. target strain for several control approaches and target strain magnitudes.

terms of magnitude, when the hysteresis behavior is the most important, especially for the analytical inversion of the linear direct model. Furthermore, the hysteresis is almost totally suppressed using the bi-exponential fit of the voltage derivative-strain derivative coefficient β, although minor overestimation of the required voltage and thus higher strain than targeted appears at low driving magnitudes. Even if the models were mainly fitted regarding the high voltage/strain response, the strain output is still well reconstructed with respect to the target one whatever the driving magnitude, thanks to the control principles whose experimental evidence is given in Figure 3. Hence, such results demonstrate the efficiency of the proposed inverse model for obtaining target strain using simple yet effective system-level hysteresis modeling approach. As highlighted by Table 2, while inverse linear approach slightly outperforms the bi-exponential inverse method at low magnitude in terms of maximal strain value (which can be explained by the fact that bi-exponential inverse model parameter set was mainly identified considering high magnitude case), the latter allows a drastic reduction of the hysteresis behavior, making it more suitable for precise control.

Experimental driving voltages are depicted in Figure 8. As expected, the direct control voltage is a direct image of the target strain (*i.e.*, unipolar sine) that therefore cannot correctly control the hysteretic behavior of the transducer. Compared to the inverse linear and bi-exponential inverse models, it can be seen that the direct control voltage magnitude is lower at low strain magnitudes and higher at high strain magnitudes, which is consistent with the strain results of Figure 7. Such an effect is actually caused by an underestimation of the voltage derivative-strain derivative coefficient β at low strain values and by its overestimation at high target strain values. On the other hand, control signals based on inverse models are not only able to adapt their magnitude,

		Direct	Inverse linear	Bi-exponential inverse
200 μdef target magnitude	Max strain (error)	181 μdef (−9.4%)	213 μdef (+6.5%)	221 μdef (+10.5%)
	Hysteresis area (reduction w.r.t. direct control)	2 725 μdef^2 (N/A)	1 758 μdef^2 (35.5%)	922 μdef^2 (66.2%)
500 μdef target magnitude	Max strain (error)	529 μdef (+5.9%)	522 μdef (+4.5%)	524 μdef (+4.8%)
	Hysteresis area (reduction w.r.t. direct control)	30 218 μdef^2 (N/A)	7 960 μdef^2 (73.7%)	2 639 μdef^2 (91.2%)
800 μdef target magnitude	Max strain (error)	905 μdef (+13.1%)	791 μdef (−1.1%)	796 μdef (−0.5%)
	Hysteresis area (reduction w.r.t. direct control)	85 743 μdef^2 (N/A)	6 714 μdef^2 (92.2%)	2 926 μdef^2 (96.6%)

Table 2: Quantitative comparison of the considered schemes.

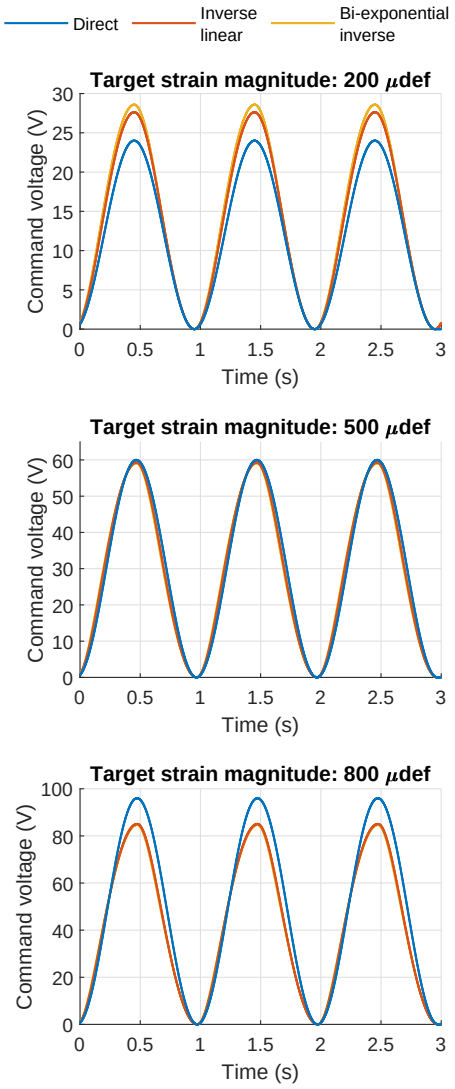

Figure 8: Experimental voltage waveforms for several control approaches and target strain magnitudes.

but also their shape as the associated waveforms are no longer pure sine, with a dissymmetrical shape that becomes more and more pronounced as the target strain magnitude increases, hence efficiently addressing the hysteresic behavior of the transducer thanks to the evolution of β with the desired target strain value (contrary to the direct control where β is fixed).

5.4. Case of advanced signals

While the previous developments and validations considered pure sinusoidal signals, it is proposed here to evaluate through numerical simulations the performance of the proposed scheme when the target strain waveform is more complex. To do so, a discrete Preisach model of the actuator is considered (such an approach is preferred here to the previously validated direct model ([29]) in order to exclude any biased result as the inverse model is initially based on the latter). The control system (using bi-exponential inverse model through the function h) is then implemented

to feed the obtained transducer block, leading to the representation shown in Figure 9. For comparison purposes, the direct control is also implemented, with the gain fixed as the inverse linear (low magnitude) gain of the actuator model.

The first simulation consisted in a triangular command strain with an intermediate magnitude of 400 μdef. The interest in this waveform, in addition to its wide use, is the fact that the triangular function shows a discontinuous derivative, along with no exact zero crossing. However, as depicted in Figure 10(a), the response of the device using the proposed inverse model still allow a faithful output strain compared to the target one, with a maximal error of less than 3%.

Another signal under consideration lies in an abruptly changing (decreasing) target strain magnitude, allowing the appearance of minor loops in the hysteretic response. Results, depicted in Figure 10(b), also show a good strain control. However, after the appearance of the minor cycle, it can be noted that a small static error appears. This could be explained by the abrupt change, especially in the input command strain derivative. Indeed, one limitation of the proposed model lies in the use of an integral form to get the required voltage (as the method is based on the coefficient linking strain and voltage derivatives), which is therefore quite sensitive to initial conditions and abrupt changes. However, in real applicative environments, natural filtering would prevent such sudden modification of signals, while the control system should have sufficiently small sampling rate to avoid aliasing.

Finally, Figure 11 depicts the response to a step input[6]. It should however be noted here that the transducer model does not relate the dynamic response of the real transducer, which is nonetheless out of the scope of the present study. Compared to the direct control case, which yields increasing error with the command strain magnitude due more pronounced hysteresis effect, it can be seen than the proposed model, taking into account such a nonlinearity, permits drastically

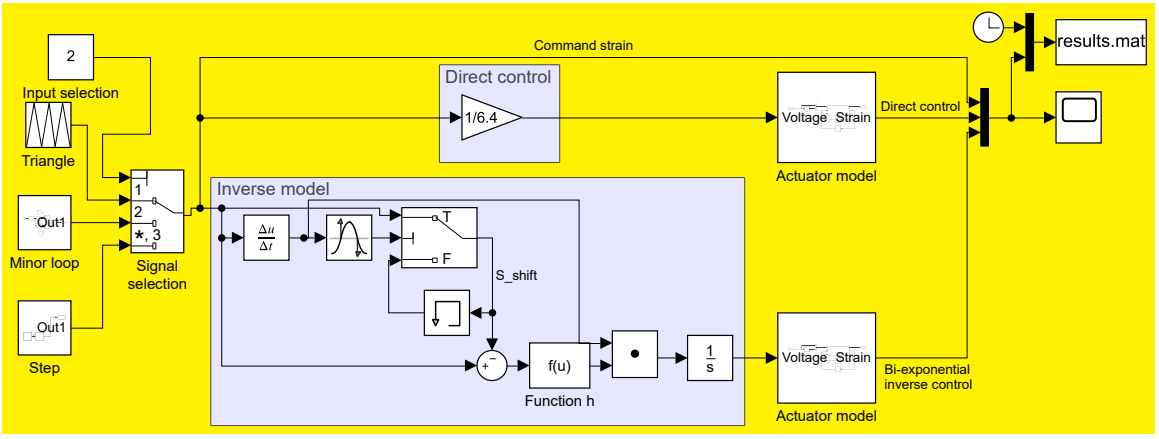

Figure 9: Simulink model for the assessment of advanced target strain waveforms.

[6]In order to keep the simulation meaningful and not prone to purely numerical divergence, the step response has been affected by a slew rate of 10^4 μdef.s^{-1}.

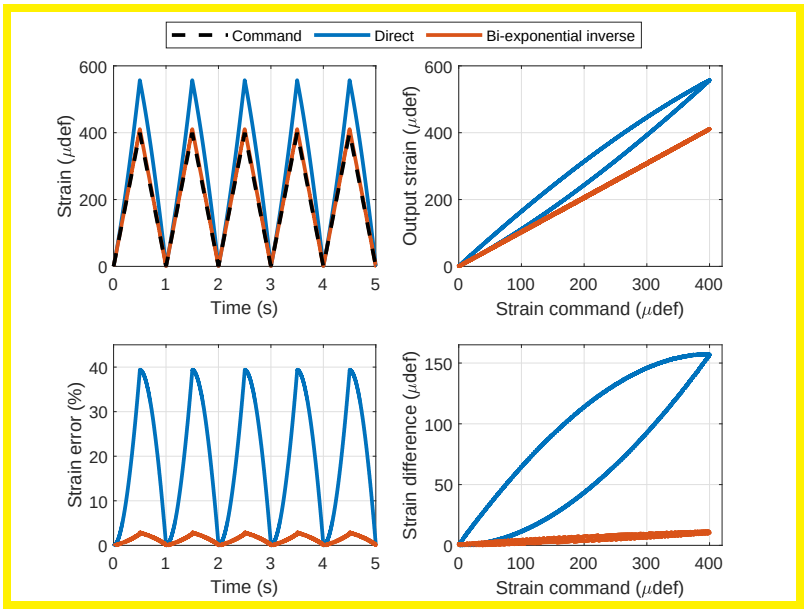

(a) Triangular strain

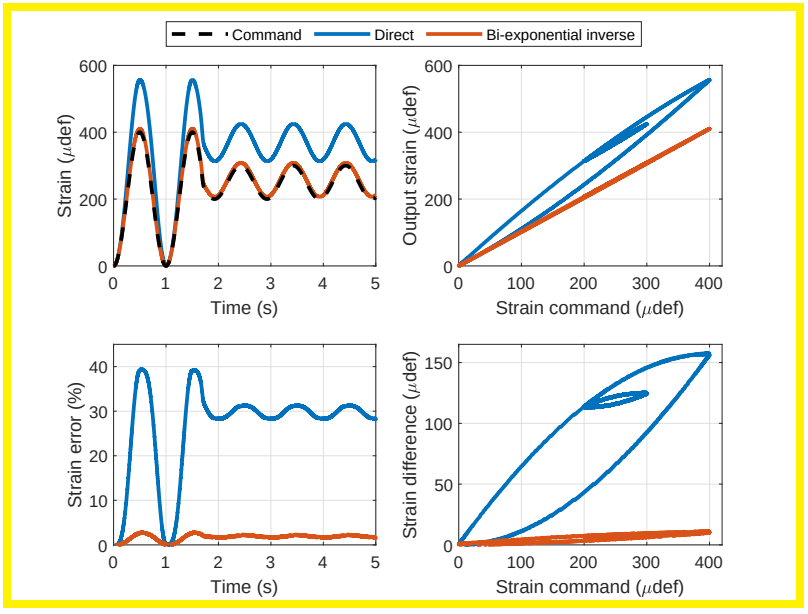

(b) Strain featuring abrupt magnitude change

Figure 10: Responses to a) Triangular target strain and b) target strain with abruptly varying magnitude (minor cycles).

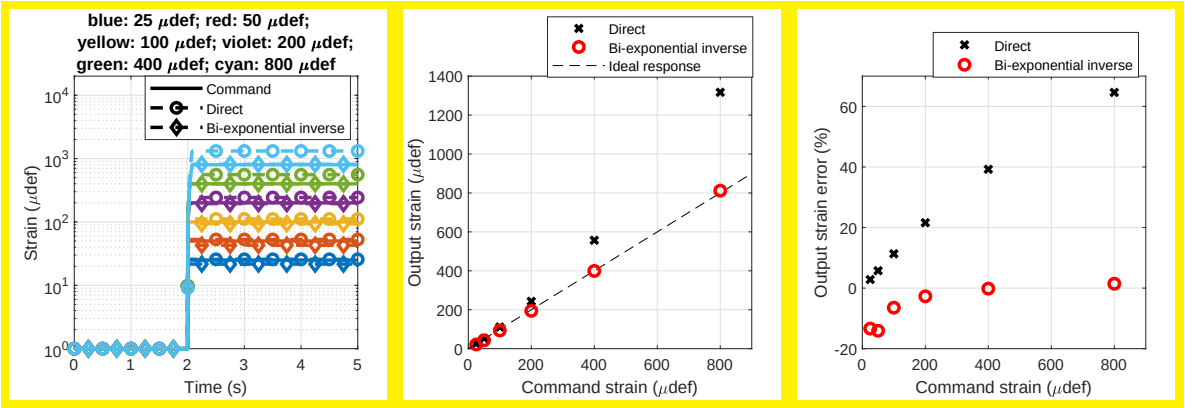

(a) Time domain waveforms (b) Maximal strain vs. maximal command strain (c) Strain error vs. maximal command strain

Figure 11: Response to step strain input.

limiting the error, hence providing output strain very close to the target one (Figure 11(b)). An underestimation can however be noticed at small driving magnitude, with an error of about 15% at small driving strains (while this error stays under 5% for strain magnitudes above 200 μdef - Figure 11(c)). Such a deviation can be attributed to the selected bi-exponential function and the associated fitted parameter sets. More particularly, at small strains, as the exponential terms approach 1, the sum of the two pre-exponential factors should be equal to the small-signal direct gain, which is not the case when using the previously fitted parameters, that are more adapted to medium to high strain magnitudes. In other words, the main limiting factor in this case of small-signal excitation arises from the choice of the function h' (and associated parameters) rather than the root principles of the proposed model.

6. Conclusion

Based on an computationally and memory efficient yet effective direct hysteresis model, the present study proposed an open-loop, system-level quasi-static control technique for a hysteretic piezoelectric actuator by developing an inverse approach based on rather similar principles as the direct model. These principles lie in the consideration of the coefficient linking the required driving voltage derivative to the target strain derivative. More precisely, this coefficient is calculated according to a mathematical function that is shifted and inverted when the target strain derivative crosses zero value, with the shifting strain being the target strain value when its derivative crosses zero. While the two models (direct and inverse) feature rather different physical roots, objectives and methods, the rather similar methodology for both of them demonstrates the strong advantage of such an approach for providing unified concepts.

Analytically derived and experiment-based inverse model applications have also been experimentally implemented in the framework of the quasi-static control of a piezoelectric transducer

strain in a successful way, yielding a very good linear relationship between the target and measured strains, both in terms of hysteresis reduction and magnitude matching. Hence, such an approach can be of significant interest to dispose of a computationally and memory efficient (as it only requires few parameters and one storing variable) yet effective model to be implemented into embedded control systems. Finally, although the model has been demonstrated on a piezoelectric transducer, its principles can be extended to any kind of actuators (electromagnetic or magnetorheological for instance). Further works would consist in including loading effects as well as dynamic contributions such as (potentially nonlinear) dynamic losses, creep and so on, to further extend the model accuracy and applicability.

References

[1] S. O. R. Moheimani and G. C. Goodwin, "Guest Editorial - Introduction to the Special Issue on Dynamics and Control of Smart Structures", *IEEE Trans. Cont. Syst. Tech.*, Vol. 9(1), pp. 3-4, 2001.

[2] S. S. Aphale, A. J. Fleming and S. O. R. Moheimani, "Integral control of smart structures with collocated sensors and actuators", *Proc. Eur. Cont. Conf. 2007*, Kos, Greece, July 2-5, 2007, pp. 2595-2602, 2007.

[3] G. Liu and H. Cao, "Design, Controlling and Detection of Smart Structures ", *2011 International Conference on Electronics and Optoelectronics (ICEOE 2011)*, Dalian, China, July 29-31, 2011, pp. V4-385-V4-388, 2011.

[4] M. Collet, M. Ouisse and F. Tateo, "Adaptive Metacomposites for Vibroacoustic Control Applications", *IEEE Sensors*, Vol. 14(7), pp.2145-2152, 2014.

[5] L. Riccardi, G. Rizzello, D. Naso, B. Holz, S. Seelecke, H. Janocha and B. Turchiano, "Modeling and Control of Innovative Smart Materials and Actuators: A Tutorial", *2014 IEEE Conference on Control Applications (CCA)*, October 8-10, 2014. Antibes, France, pp. 965-977, 2014.

[6] W.-G. Drossel, H. Kunze, A. Bucht, L Weisheit and K. Pagel, "Smart^3 - Smart Materials for Smart Applications", *Proc. CIRP*, Vol. 36, pp. 211-216, 2015.

[7] T. Zhang, H. G. Li and G. P. Cai, "Hysteresis identification and adaptive vibration control for a smart cantilever beam by a piezoelectric actuator", *Sens. Act. A: Phys.*, Vol. 203, pp. 168–175, 2013.

[8] K. Saigusa and T. Morita, "Self-sensing control of piezoelectric positioning stage by detecting permittivity", *Sens. Act. A: Phys.*, Vol. 226, pp. 76–80, 2015.

[9] P.-B. Nguyen, S.-B. Choi and B.-K. Song, "A new approach to hysteresis modelling for a piezoelectric actuator using Preisach model and recursive method with an application to open-loop position tracking control", *Sens. Act. A: Phys.*, Vol. 270, pp. 136–152, 2018.

[10] J. Li, H. Huang and T. Morita, "Stepping piezoelectric actuators with large working stroke for nano-positioning systems: A review", *Sens. Act. A: Phys.*, Vol. 292, pp. 39–51, 2019.

[11] V. Hassani, T. Tjahjowidodo and T .N. Do, "A survey on hysteresis modeling, identification and control", *Mech. Syst. Sig. Proc.*, Vol. 49, pp. 209-233, 2014.

[12] F. Preisach, "Uber die magnetische nachwirkung", *Zeitschrift fur Physik*, vol. 94, pp. 277-302, 1935.

[13] M. A. Krasnosel'Skii and A. Pokrovskii, "Systems with Hysteresis", Springer-Verlag, 1989.

[14] X. Liu, Y. Wang, J. Geng, Z. Chen, "Modeling of hysteresis in piezoelectric actuator based on adaptive filter", *Sens. Act. A: Phys.*, Vol. 189, pp. 420–428, 2013.

[15] Y. Dong, H. Hu and H. Wang, "Identification and experimental assessment of two-input Preisach model for coupling hysteresis in piezoelectric stack actuators", *Sens. Act. A: Phys.*, Vol. 220, pp. 92–100, 2014.

[16] F. Al-Bender, V. Lampaert and J. Swevers, "The generalized Maxwell-slip model: a novel model for friction Simulation and compensation", *IEEE Trans. Autom. Cont.*, vol. 50(11), pp. 1883-1887, 2005.

[17] K. Worden, C. X. Wong, U. Parlitz, A. Hornstein, D. Engster, T. Tjahjowidodo, F. Al-Bender, D. D. Rizos and S. D. Fassois, "Identification of pre-sliding and sliding friction dynamics: Grey box and black-box models", *Mech. Syst. Sig. Proc.*, Vol. 21, pp. 514-534, 2007.

[18] M. Lallart, G. Sebald, J.-F. Capsal, B. Ducharne and D. Guyomar, "Modeling of hysteretic behavior in ferroelectric polymers", *J. Pol. Sci. p. B: Pol. Phys.*, vol. 54, pp. 499–508, 2016.

[19] D. C. Jiles and D. L. Atherton, "Theory of the Magnetisation Process in Ferromagnets and its Application to the Magnetomechanical Effect", *J. Phys. D: Appl. Phys.*, vol. 17, pp. 1265-1281, 1984.

[20] D. C. Jiles and D. L. Atherton, "Theory of ferromagnetic hysteresis (invited)", *J. Appl. Phys.*, vol. 55, pp. 2115-2120, 1984.

[21] J. V. Leite, N. Sadowski, P. Kuo-Peng and A. Benabou," Minor Loops Calculation with a Modified Jiles-Atherton Hysteresis Model", *J. Microwaves, Optoelec. Electromag. Appl.*, Vol. 8(1), pp. 49S-55S, 2009.

[22] R. Bouc, "Forced vibration of mechanical systems with hysteresis", in *Proceedings of the Fourth Conference on Nonlinear Oscillation*, Prague, Czechoslovakia, 1967, p. 315.

[23] Y. K. Wen, "Method for random vibration of hysteretic systems", *J. Eng. Mech.*, Vol. 102(2), pp. 249-263, 1976.

[24] G. Wang, G. Chen, F. Bai, "Modeling and identification of asymmetric Bouc–Wen hysteresis for piezoelectric actuator via a novel differential evolution algorithm", *Sens. Act. A: Phys.*, Vol. 235, pp. 105–118, 2015.

[25] P. Duhem, "Die dauernden Aenderungen und die Thermodynamik," I, *Z. Phys. Chem.*, vol. 22, pp. 543-589, 1897.

[26] M. F. M. Naser and F. Ikhouane, "Characterization of the Hysteresis Duhem Model," *Proc. 5th IFAC International Workshop on Periodic Control Systems*, July 3-5, 2013. Caen, France, 2013.

[27] G. Wang, G. Chen, "Identification of piezoelectric hysteresis by a novel Duhem model based neural network", *Sens. Act. A: Phys.*, Vol. 264, pp. 282–288, 2017.

[28] W. Li, X. Chen, "Compensation of hysteresis in piezoelectric actuators without dynamics modeling", *Sens. Act. A: Phys.*, Vol. 199, pp. 89–97, 2013.

[29] M. Lallart, K. Li, Z. Yang and W. Wang, "System-level modeling of nonlinear hysteretic piezoelectric actuators in quasi-static operations", *Mech. Syst. Sig. Proc.*, Vol. 116, pp. 985-996, 2019.

[30] M. Rakotondrabe, "Bouc-Wen modeling and inverse multiplicative structure to compensate hysteresis nonlinearity in piezoelectric actuators", *IEEE Trans. Autom. Sci. Eng.*, Vol. 8(2), pp. 428-431, 2011.

[31] D. Davino, Krejčí and C. Visone, "Handling Memory Properties of Smart Materials: a Review on Modeling, Compensation and Control", *2013 American Control Conference (ACC)*, Washington, DC, USA, June 17-19, 2013, pp. 3599-3604, 2013.

[32] R. Changhai and S. Lining, "Hysteresis and creep compensation for piezoelectric actuator in open-loop operation", *Sens. Act. A: Phys.*, Vol. 122, pp. 124–130, 2005.

[33] R. V. Iyer and X. Tan, "Control of Hysteretic Systems Through Inverse Compensation", *IEEE Cont. Syst. Mag.*, Vol.29(1), pp. 83-99, 2009.

[34] A. Milecki and M. Pelic, "Application of geometry based hysteresis modelling in compensation of hysteresis of piezo bender actuator", *Mech. Syst. Sig. Proc.*, Vol. 78, pp. 4-17, 2016.

[35] J. Li and H. Tian, "Position control of SMA actuator based on inverse empirical model and SMC-RBF compensation", *Mech. Syst. Sig. Proc.*, Vol. 108, pp. 203-215, 2018.

[36] A. G. Hatch, R. C. Smith, T. De and M. V. Salapaka, "Construction and Experimental Implementation of a Model-Based Inverse Filter to Attenuate Hysteresis in Ferroelectric Transducers", *IEEE Trans. Cont. Syst. Tech.*, Vol. 14(6), pp. 1058-1069, 2006.

[37] L. Riccardi, D. Naso, B. Turchiano and H. Janocha, "Design of Linear Feedback Controllers for Dynamic Systems With Hysteresis", *IEEE Trans. Cont. Syst. Tech.*, Vol. 22(4), pp. 1268-1280, 2014.

[38] S. Z. Mansour, R. Seethaler and A. Fleming, "A Simple Asymmetric Hysteresis Model for Displacement-Force Control of Piezoelectric Actuators", *Proc. of the 2018 IEEE/ASME International Conference on Advanced Intelligent Mechatronics (AIM)*, pp. 87-90, Auckland, New Zealand, July 9-12, 2018.

[39] M. Butcher, A. Giustiniani and A. Masi, "On the identification of Hammerstein systems in the presence of an input hysteretic nonlinearity with nonlocal memory: Piezoelectric actuators - an experimental case study", *Physica B: Condensed Matter*, Vol. 486, pp. 101-105, 2015.